Modeling distributions of flying insects: Effective attraction radius of pheromone in two and three dimensions

John A. Byers *

US Arid-Land Agricultural Research Center, USDA-ARS, 21881 North Cardon Lane, Maricopa, AZ 85238, USA

ABSTRACT

The *effective attraction radius* (EAR) of an attractive pheromone-baited trap was defined as the radius of a passive "sticky" sphere that would intercept the same number of flying insects as the attractant. The EAR for a particular attractant and insect species in nature is easily determined by a catch ratio on attractive and passive (unbaited) traps, and the interception area of the passive trap. The spherical EAR can be transformed into a circular EAR_c that is convenient to use in two-dimensional encounter rate models of mass trapping and mating disruption with semiochemicals to control insects. The EAR_c equation requires an estimate of the effective thickness of the layer where the insect flies in search of mates and food/habitat. The standard deviation (SD) of flight height of several insect species was determined from their catches on traps of increasing heights reported in the literature. The thickness of the effective flight layer (F_L) was assumed to be $SD \cdot \sqrt{2 \cdot \pi}$, because the probability area equal to the height of the normal distribution,$1/(SD \cdot \sqrt{2 \cdot \pi})$, times the F_L is equal to the area under the normal curve. To test this assumption, 2000 simulated insects were allowed to fly in a three-dimensional correlated random walk in a 10-m thick layer where an algorithm caused them to redistribute according to a normal distribution with specified SD and mean at the midpoint of this layer. Under the same conditions, a spherical EAR was placed at the center of the 10-m layer and intercepted flying insects distributed normally for a set period. The number caught was equivalent to that caught in another simulation with a uniform flight density in a narrower layer equal to F_L, thus verifying the equation to calculate F_L. The EAR and F_L were used to obtain a smaller EAR_c for use in a two-dimensional model that caught an equivalent number of insects as that with EAR in three dimensions. This verifies that the F_L estimation equation and EAR to EAR_c conversion methods are appropriate.

Published by Elsevier Ltd.

1. Introduction

Simulation of mating disruption and mass trapping of insects based on individual movements of insects (Turchin, 1998) responding to attractive chemicals released in plumes downwind would aid development of successful control programs (Cardé, 1990; El-Sayed et al., 2006; Miller et al., 2006a, b; Byers, 2007, 2008). One parameter that relates to such models is the *active space*, defined by Elkinton and Cardé (1984) as the volume of air inside which the odor concentration is above the threshold that elicits a behavioral reaction in the receiving organism (Sower et al., 1971; Nakamura and Kawasaki, 1977; Baker and Roelofs, 1981). Behavioral chemicals released from a dispenser begin to diffuse as they are transported downwind with turbulence increasing spread as described moderately well by Gaussian

plume models (Bossert and Wilson, 1963; Sutton, 1953; Fares et al., 1980; Elkinton and Cardé, 1984; Elkinton et al., 1984). The fine-structure of pheromone plumes on a small time scale is complicated but thought to be comprised of filaments of higher concentrations due to turbulent eddies of air (Mankin et al., 1980; Elkinton and Cardé, 1984; Baker et al., 1998). At some distance downwind, the concentration becomes less than what the insect can detect (Fig. 1A).

The active space has been investigated by observing male moths fanning their wings inside cages at various points downwind within a pheromone plume (Elkinton and Cardé, 1984; Elkinton et al., 1984). While plumes and active spaces are three-dimensional (3D) in nature, they can be simplified to two dimensions because mate- and host-seeking insects disperse and orient over hundreds of meters within a relatively thin layer of air a few meters thick (e.g., Chisholm et al., 1979; Ladd and Klein, 1982; Proshold et al., 1986; D'Arcy-Burt and Blackshaw, 1987; Gillespie and Vernon, 1990; Robacker et al., 1990; Valles et al., 1991; Diraviam and Uthamasamy, 1992; Youm and Beevor, 1995; Critchley et al., 1997; Ruther, 2004). The plume's active

* Tel.: +1 502 316 6339; fax: +1 520 316 6330.
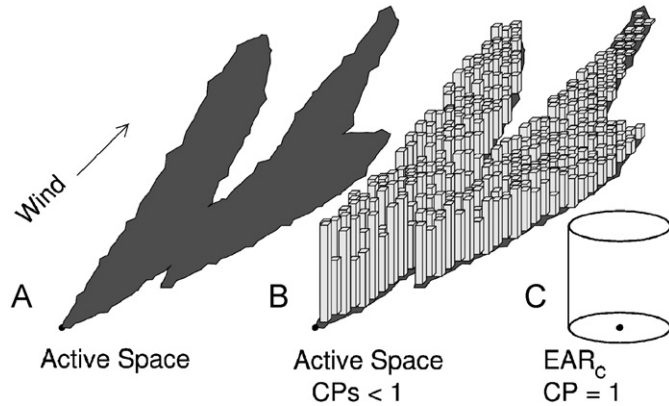E-mail address: John.byers@ars.usda.gov

Fig. 1. (A) Representation of a pheromone plume as an active space in which semiochemical concentration is above a behavioral threshold eliciting orientation, (B) the same plume represented with CP (capture probabilities <1) indicating the probability of an insect reaching the pheromone source upon initial observation at a particular position, (C) the capture finding probability surface compressed into an EAR_c (effective attraction radius) with the same effect on catch by reducing the diameter but maximizing the CP at a probability of one.

Fig. 2. The spherical effective attraction radius ($EAR = 1.009$ m) in three dimensions calculated by the cylindrical interception area as seen from one side (0.16 m^2) and the ratio of catch (20) of attractive and passive sticky traps (Eq. (1)). The spherical EAR in an effective flight layer (F_L) of 4 m then can be converted (Eq. (5)) into an equivalent circular EAR_c (0.4 m) for use in two-dimensional models.

space is affected by wind speed, turbulence, temperature, topography, vegetation, and time scale (Elkinton and Cardé, 1984; Elkinton et al., 1984; Byers, 1987). Thus, under field conditions the active space might be at least as chaotic as suggested in Fig. 1A.

To complicate matters, a *capture probability* (CP) is assumed in which there would be a specific CP at any position in the active space (McClendon et al., 1976; Wall and Perry, 1987; Branco et al., 2006). The CP depends on the semiochemical blend concentration, wind conditions, distance from source, and orientation ability of the insect species (Fig. 1B). It is well known from theoretical and experimental studies such as those above that concentration of odor declines with distance from the source, and also that at low release rates insects are less attracted (e.g., Byers et al., 1988). This is probably due to a combination of more individual variation in response threshold, lower frequency of action potentials from receptor neurons, and lower plume filament flux frequency at these low concentrations (Baker et al., 1998). Therefore, we expect that insects entering the active space of a plume at a position far from the source would have a lower probability of finding the source than an insect entering much nearer to the source. For example, McClendon et al. (1976) presented a capture probability response surface based on catch of marked boll weevils, *Anthonomus grandis* Boheman, released at various distances from a synthetic pheromone source. The probabilities ranged from 5% at about 150 m from the source to about 45% near the source. Thus, the CP depends on where the insect enters the active space (Fig. 1B).

There is a substitute for the active space-CP response surface of the plume that is much easier to delineate based on field catches. The *effective attraction radius* (EAR) proposed by Byers et al. (1989) is the radius of a passive sphere that would intercept the same number of insects as a specific attractive trap baited with semiochemicals. The EAR is easily determined by a time-averaged catch ratio of traps in the field (Fig. 2). Of particular importance is that the EAR at different population densities should give the same value because it is derived from a ratio of catches (Byers et al., 1989). A similar concept used in models of insect mate finding, mass trapping, and host tree finding (Byers, 1991, 1993, 1996, 1999) is termed the EAR_c (c for circle) to distinguish it from the spherical EAR. In the EAR_c used in models, all the various CP within the active space are compressed into a circular area with a CP equal to one that insects entering will find the source and be
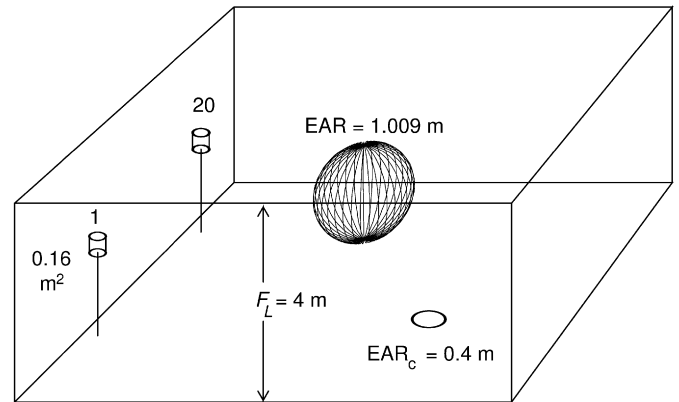
trapped (Figs. 1C and 2). These and other models use individual-based movements of animals (Turchin, 1998) moving in a *correlated random walk* (CRW). In contrast to molecular diffusion that is random, animals disperse in a CRW with forward direction because the direction of each step is correlated to some degree with their previous step direction (Byers, 2001).

Byers (2008) showed that a suitably sized EAR_c would catch the equivalent to an active space-CP plume of any size or complexity. He derived equations that would convert the EAR of field catches to the EAR_c of models. However, the conversion requires knowledge of the effective flight layer. A number of studies have sampled flight heights of insects with a series of traps placed vertically above the ground (e.g., Ficht and Hienton, 1941; Rothschild and Minks, 1977; Meyerdirk et al., 1979; Dix et al., 1979; Snow, 1982; Elliott et al., 1986; Byers et al., 1989; David and Horsburgh, 1989; McPherson and Weber, 1990; Peng and Williams, 1991; Weissling and Meinke, 1991; McPherson et al., 1993; Ware and Compton, 1994; and more references in Table 2). Most of these studies do not report the mean flight height or *SD*. My first objective was to analyze previous studies for mean flight height and *SD*, and then convert this to the effective flight layer, F_L. This layer of uniform flight density is assumed to be equivalent to a normal distribution of the observed mean catch for purposes of transforming the EAR to EAR_c. My second objective was to simulate a normal distribution of insects in flight within a 3D area with a spherical trap (EAR) and determine the catch. Then I wanted to calculate the *SD* of this simulated flight distribution in order to calculate a F_L and convert the spherical trap radius to an EAR_c. If this EAR_c caught an equivalent number in two dimensions then this would confirm the conversion formula of EAR to EAR_c as well as the equation determining F_L.

2. Methods

2.1. EAR and EAR_c equations

The original EAR, proposed by Byers et al. (1989), was the radius of a sphere as calculated by the equation:

$$EAR = \sqrt{\frac{A_c \cdot 2 \cdot r \cdot h}{P_c \cdot \pi}} \tag{1}$$

where A_c is the catch on the active trap (semiochemical), P_c is the catch on the passive (unbaited) trap, and r is the radius and h is the height of the passive trap cylinder (interception area as seen

from one direction). For hanging flat panel traps of width x height, $2 \cdot r \cdot h$ in Eq. (1) can be substituted with the average trap interception area T_A:

$$T_A = height \cdot width \cdot \int_0^{\pi/2} \frac{2 \cos(x)}{\pi} \, dx$$
$$= height \cdot width \cdot 0.637 \tag{2}$$

(Byers et al., 1989). Cross-vane traps have an average trap interception area of:

$$T_A = height \cdot width \cdot \int_0^{\pi/4} \frac{4 \cos(x)}{\pi} \, dx$$
$$= height \cdot width \cdot 0.9 \tag{3}$$

In simulation models, the EAR is better described as the radius of a circle or cylinder:

$$EAR_c = \frac{A_c \cdot T_A/2}{P_c \cdot F_L} \tag{4}$$

where F_L is the thickness of the air layer in which insects primarily search while flying.

Substituting Eq. (1) into Eq. (4) gives:

$$EAR_c = \frac{\pi \cdot EAR^2}{2 \cdot F_L} \tag{5}$$

(Byers, 2008) which coverts EAR to EAR_c when F_L is estimated in the next section.

The EAR values of the bark beetles, *Ips typographus* (L.), *I. paraconfusus* Lanier, and *Tomicus piniperda* (L.), for various aggregation pheromone baits and attractive host tree logs were calculated from published results using Eq. (1) and converted to EAR_c values with Eq. (5). Similarly, EAR/EAR_c values were calculated from published results of catches of western flower thrips, *Frankliniella occidentalis* (Pergande) on attractive blue, yellow or white sticky cards compared to non-attractive green and black cards.

2.2. Mean flight height±standard deviation (SD) from field studies and estimating F_L

The scientific literature was searched (BIOSIS Previews) for articles on flight heights of insects caught by traps to determine the mean height of flight and SD (McCall, 1970; Byers, 2008) needed to estimate the effective flight layer of search, F_L (presented subsequently). In addition, catches on attractant and passive sticky traps were used to estimate EAR from Eq. (1) and EAR_c from Eq. (4). The maximum height of the normal curve occurs at $x = \mu$ (the mean) which reduces to:

$$Y = \frac{e^{-(x-\mu)^2/2 \cdot SD^2}}{SD \cdot \sqrt{2 \cdot \pi}} = \frac{1}{SD \cdot \sqrt{2 \cdot \pi}} \tag{6}$$

where SD is the standard deviation of the flight distribution. Thus, the height of the normal curve at the mean times the value in the denominator will give a value of one which is the area under the curve. Therefore, the density distribution under the normal curve is equivalent to a flight layer of uniform density, F_L, as given by:

$$F_L = SD \cdot \sqrt{2 \cdot \pi} \tag{7}$$

However, Eqs. (5) and (7) need to be validated by simulations in three dimensions to evaluate catch on an EAR under various SD of mean flight height and estimated F_L (in Sections 2.3 and 2.4). This would then be followed by conversion of the EAR to EAR_c and subsequent simulation in two dimensions that should give the same catch if the equations are valid (in Section 2.5).

2.3. Simulation of insect movement and flight distribution in three dimensions

Insects were simulated in a 3D area with x-axis (xa), y-axis (ya), and z-axis (za) that can be adjusted but were held at $20\,m \times 20\,m \times 10\,m$, respectively, in which a spherical EAR was centered at ($xa/2$, $ya/2$, $za/2$). Insects flew within the volume according to a CRW under rules that resulted in a normal distribution of densities with SD centered about the mean flight height ($za/2$) as explained subsequently. Each insect was given an initial direction and (x, y, z) position at random, thereafter each insect followed a CRW made of a series of steps each of length *step* (usually 0.1 m). Spherical coordinates (Hearn and Baker, 1994) were calculated at each insect step as a 3D vector from the former position (x_0, y_0, z_0), $x_1 = x_0 \cdot s \cos(\theta)\sin(\phi)$, $y_1 = y_0 \cdot s \sin(\theta)\sin(\phi)$, and $z_1 = z_0 \cdot s \cos(\phi)$ based on the former direction plus random angular changes in the directional angles (θ, ϕ). Thus, $\theta = \theta + \alpha$ (if $\theta > 2\pi$ then $\theta = \theta - 2\pi$, if $\theta < 0$ then $\theta = \theta + 2\pi$) and $\phi = \phi + \beta$ (if $\phi > \pi$ then $\phi = \phi - \pi$, if $\phi < 0$ then $\phi = \phi + \pi$), where α and β were chosen at random from a normal distribution with a $6°$ SDA (standard deviation of angular turns as in Byers, 2001). In addition, the (x, y, z) coordinates were transformed to 3D perspective coordinates when viewing the simulations (Adams, 1987, p. 57).

When insects were placed initially at random uniformly throughout the 3D space (with rebound at random at boundaries), the population soon moved such that individuals were distributed according to a normal distribution with mean height at $za/2$ and specified SD, as accomplished by the following simple algorithm. If the insect is above the mean ($za/2$) then $\phi = \phi - \omega$, while if below the mean then $\phi = \phi + \omega$, and then if $\phi > \pi$ then $\phi = \pi$ and if $\phi < 0$ then $\phi = 0$, where $\omega =$ an incremental turn angle in radians that depended on which step size and SDA were used and which SD was desired. Thus, ω was varied for several sets of SDA (3–12°), step (0.05–0.2 m), and SD (0.5–2.5 m), to empirically find sets with the lowest Chi-square when comparing histograms of insect numbers in 18 successive height levels in the volume to expected values based on a normal distribution of SD (McCall, 1970). The best fitting curvilinear regression was performed on SD versus the optimized ω.

The model was programmed in QuickBASIC 4.5 (Microsoft Corp., Redmond, WA) for use in simulations as well as Java 2.1 (Sun Microsystems Inc., Santa Clara, CA) for general demonstration on the Internet with a web browser (http://www.chemical-ecology.net/java2/sd-3d.htm).

2.4. Simulation of insect movement and catch on EAR in three dimensions

The same model as above was used to simulate vertical flight distributions of various SD as set up by steps of 0.1 m each (SDA = 6°) and $\omega = 0.0715$ radians (Fig. 3). Then, a spherical EAR of 0.5 m radius or similar was placed at 5 m height in the center of the flight volume and 2000 insects were released uniformly in the volume to redistribute according to a normal distribution (Fig. 3) while the number caught on the EAR sphere over a limited time, usually 720 steps, was recorded (eight simulations for each set of variables). The algorithm to determine whether insects entered or passed through the spherical EAR in 3D during a step from (x, y, z) to (p, q, r), i.e., were caught, was modified from that in Byers (1991, Fig. 3), for a circle in two-dimensions (2D). In the 2D algorithm, the EAR's (j, k) coordinates are compared to the insect's step from (x, y) to (p, q) coordinates in the x–y plane. Thus, by repeating the algorithm for the x–z plane (from x, z to p, r) and y–z plane

```
10   56      actual mean height= 5.061254  sd= 1.659529        3D MASS
9    44      actual FL= 4.159823                               TRAPPING
8    99      10-trap mean height= 5.0795  sd= 1.665253          rebound
7    263     trap est. FL= 4.17417                             MOVES:
6    564                                                           360
5    573                                                        of 360
4    251
3    61                                                        Traps= 1
2    45                                                        radius=1
1    44                                                        seed=10
                                                               Bugs= 2000
                                                               speed (m/s)=
                                                                  .1
                                                               step= .1
                                                               SD° = 6°
                                                               x= 20
                                                               y= 20
                                                               z= 10
                                                               sd= 1.666667
                                                               FL= 4.177714
                                                               za= .08
                                                               Catch:
                                                                 157
                                                               Time left=
                                                                 0
                                                                per km² :
                                                               bugs=
                                                               1E+07
                                                               traps=
                                                               5000
```
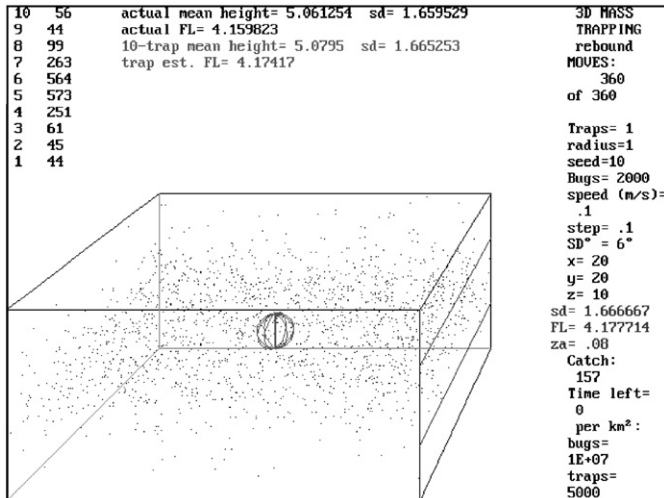
Fig. 3. Simulation screen showing spherical EAR in a $20 \times 20 \times 10$ m three-dimensional space in which individual insects can fly anywhere but the population distributes according to a normal distribution of specified standard deviation (*SD*).

(from y, z to q, r), then any interception of a sphere by an insect during a step can be determined.

Because equilibrium takes a short time to obtain a specified normal distribution, this potential error was minimized by initially placing insects at random according to the specified normal distribution of *SD*. This was done by selecting a z-coordinate uniformly at random from 0 to *za*. Then, if a uniform random number (0 to 1) times the second part of Eq. (6) was less than the first part of Eq. (6), where $z = x$, then z was chosen as a coordinate, otherwise continue random selections until the condition was met.

If Eq. (7) for F_L is valid, the catch above should be equivalent to a 3D simulation with the same number in a flight layer $= F_L$ of uniform density. Thus, Eq. (7) was used to estimate the effective F_L from the *SD*, and this F_L was used with an $\omega = 0$ (so a uniform flight density persisted) in a $20\,\text{m} \times 20\,\text{m} \times 4.17\,\text{m}$ high volume to determine whether the catch on an EAR of 0.5 m was equivalent. This catch should also be equivalent to the catch on the EAR_c in 2D according to Eq. (5) as presented subsequently.

2.5. Simulation of insect movement and catch on EAR_c in two dimensions

Insects were simulated in two dimensions with x-axis (*xa*) and y-axis (*ya*) that can be adjusted but was usually $20\,\text{m} \times 20\,\text{m}$ in which an EAR_c was placed at (*xa*/2, *ya*/2). Insects flew in the area according to a CRW as in earlier models (Byers, 1996, 1999, 2001). Each insect was given an initial direction and position at random. Thereafter each insect followed a CRW made of a series of steps of specified distance, each step calculated as a polar vector from the former position. The direction at each step was the former direction plus a turning angle chosen at random from a normal distribution, usually $6°$ *SDA*, centered on the former direction (Byers, 2001). Insects entering the EAR_c reached the source with a probability of 1, i.e. were caught. The algorithm for encountering the circle was as reported in Byers (1991). The goal was to use Eq. (5) based on the F_L and EAR catch in the 3D simulation model to predict an EAR_c in the 2D model that will catch an equivalent number. If the predicted EAR_c does catch the same then this would confirm the validity of Eq. (7) for estimating the F_L.

3. Results

3.1. EAR and EAR_C equations

There is a positive linear relationship between radius of the passive trap and the EAR of the sphere, while the EAR_c increases as a squared function of the trap radius. The exact relationship depends on the ratio of catch (active/passive), the interception area of the passive trap as seen from one direction, and in the case of the EAR_c, the effective flight layer (F_L) thickness (Fig. 4). When the EAR_c (Y) is plotted against EAR (X), the EAR_c increases as the square of the EAR ($Y = aX^2$), where $a = \pi/(2F_L)$. The relationship between EAR and EAR_c does not depend on the catch ratio or the dimensions of the passive trap, however, the thickness of F_L does influence EAR_c (Fig. 4). EAR_c and EAR usually are different in radius length except when F_L is equal to $\pi \cdot EAR/2$. The EAR values for various aggregation pheromone baits and attractive host tree logs of the bark beetles, *Tomicus piniperda*, *Ips typographus*, and *I. paraconfusus* are estimated in Table 1. In addition, this table shows EAR values for colors attractive to western flower thrips.

3.2. Mean flight height $\pm$ standard deviation (SD) from field studies and estimating F_L

Over 100 articles were found on insect flight heights of which only some were suitable for estimating the flight layer of search, F_L (Table 2). Insects attracted to colors or semiochemicals may have had their natural flight distributions altered (Table 2), however, this is unlikely for species caught by non-attractive traps (sticky screens or window barriers, Table 2). Agricultural insects of crops usually fly within a few meters above the ground. For example, the minute western flower thrips (*Frankliniella occidentalis*) that feed on vegetable crops have a mean flight height of about 2.3 m and a F_L of only about 1 m (Table 2). The important whitefly pest of numerous crops, *Bemisia tabaci*, distributed worldwide has a similar mean flight height of about 0.55 m and a narrow F_L of 0.77 m. Observations of the common sulfur (*Colias philodice* Godart) butterflies in an alfalfa field indicated that most flew within a 1 m thick layer just above the canopy. In contrast, bark beetles that search among Norway spruce and Scotch pine for susceptible hosts have a higher mean flight height of 3–7 m and F_L of 4–7 m (Table 2).
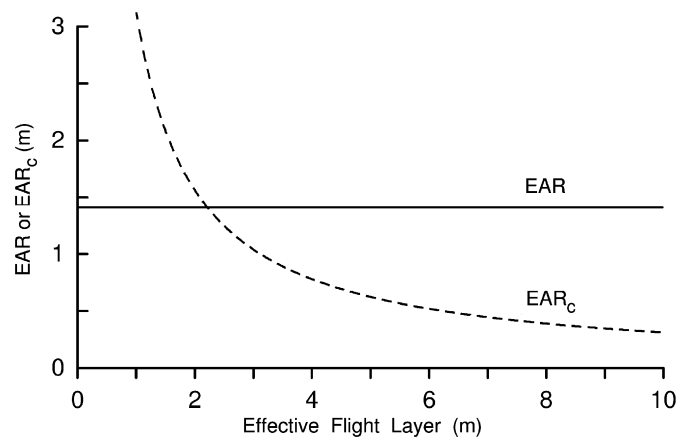

Fig. 4. EAR_c as a function of a given EAR (50:1 catch ratio on $0.125\,\text{m}^2$ trap interception area) and effective flight layer (F_L).

Table 1
EAR and EAR_c of semiochemicals attractive to bark beetles *Tomicus piniperda*, *Ips typographus*, and *I. paraconfusus* and colors attractive to western flower thrips based on passive and active catches of sticky traps and flight layer estimate (from Table 2)

Test	Insect catch		Passive trap interception area (m²)	EAR sphere (m)	Flight layer estimate (m)	EAR_c (m)
	Passive	Active				
Bark Beetles						
Tomicus piniperda						
Scots pine log I[a]	52	623	0.06	0.48	7.53	0.048
Log+30 males+30 females[a]	52	774	0.06	0.53	7.53	0.059
(+)-3-Carene[a]	7	48	0.06	0.36	7.53	0.027
(+)-α-Pinene[a]	7	60	0.06	0.40	7.53	0.034
(−)-α-Pinene[a]	7	79	0.06	0.46	7.53	0.045
Terpinolene[a]	7	104	0.06	0.53	7.53	0.059
Scots pine log II[a]	7	256	0.06	0.84	7.53	0.146
April 15, monoterpenes[b]	2.33	27	0.09	0.58	7.53	0.069
April 21, monoterpenes[b]	1	19	0.09	0.74	7.53	0.114
Ips typographus						
High release pheromone[c]	6	753	0.06	1.55	6.9	0.546
Medium release pheromone[d]	7	80	0.06	0.47	6.9	0.050
May 17, pheromone[e]	5.67	194	0.09	0.99	6.9	0.223
May 20, pheromone[e]	16.67	269	0.09	0.67	6.9	0.105
May 22, pheromone[e]	8.5	215	0.09	0.85	6.9	0.165
Ips paraconfusus						
Log+50 males[f]	1.27	339	0.1185	3.18	12.88[g]	1.233
Western flower thrips						
Frankliniella occidentalis[h]						
Blue card	29	639	0.0046	0.18	0.99	0.051
Yellow card	29	529	0.0046	0.16	0.99	0.042
White card	29	421	0.0046	0.15	0.99	0.034

[a] Released about 30 mg each compound/day; Scots pine (*Pinus sylvestris* L.); Byers et al. (1985).
[b] Released about 10–20 mg/day of (+)-α-pinene, (−)-α-pinene, and (+)-3-carene, and 3–5 mg/day of terpinolene; Byers et al. (1989).
[c] High release of 57 mg 2-methyl-3-buten-2-ol (MB)/day and 1 mg (4S)-*cis*-verbenol (cV)/day; Schlyter et al. (1987).
[d] Medium release: 5.8 mg MB/day and 1 mg cV/day; Schlyter et al. (1987).
[e] Byers et al. (1989), medium release MB and cV.
[f] Ponderosa pine log (*Pinus ponderosa* Laws.), passive catch average of 15 traps on row 3, Byers (1983).
[g] Estimate based on catches by Gara (1963).
[h] Gillespie and Vernon (1990); passive catch average of green and black sticky traps at 2.4 m height and average F_L.

Table 2
Analysis of mean height of catch $\pm SD$ (m) and effective flight layer (F_L) of various insect species calculated from catches at trap heights reported in the literature

Species	Trapping method[a]	Range of trap heights	Number of trap heights	Total catch[b]	Mean height of catch $\pm SD$	F_L (m)
Thysanoptera: Thripidae						
Frankliniella occidentalis (Pergande)[c]	Blue-St-card	0.6–3	5	858	2.32±0.41	1.03
Frankliniella occidentalis (Pergande)[c]	Y-St-card	0.6–3	5	711	2.26±0.43	1.08
Frankliniella occidentalis (Pergande)[c]	W-St-card	0.6–3	5	537	2.38±0.35	0.87
Hemiptera: Aleyrodidae						
Bemisia tabaci (Gennadius)[d]	Y-St-card	0.3–1.2	4	799	0.55±0.31	0.77
Aleurocanthus woglumi Ashby[e]	Y-St-card	0.6–6	7	439	1.59±0.72	1.81
Hemiptera: Lygaeidae						
Geocoris uliginosus (Say)[f]	Window	1–4	4	16	1.67±1.32	3.31
Pachybrachius basalis (Dallas)[f]	Window	1–4	4	31	1.36±1.56	3.91
Hemiptera: Miridae						
Lygus lineolaris (P. de Beauvois)[g]	Window	1–4	4	300	2.12±1.39	3.48
Hemiptera: Nabidae						
Nabis americoferus Carayon[f]	Window	1–4	4	26	2.75±2.29	5.74
Nabis roseipennis Reuter[f]	Window	1–4	4	73	2.58±1.88	4.71
Hemiptera: Pentatomidae						
Euschistus servus (Say)[f]	Window	1–4	4	158	1.78±1.63	4.09
Diptera: Bibionidae						
Bibio johannis (L.) males[h]	St-cylinder	0.4–1.6	3	4112	0.71±0.42	1.05
Bibio johannis (L.) females[h]	St-cylinder	0.4–1.6	3	365	0.88±0.45	1.13
Diptera: Culicidae						
Anopheles melas Theobald males[i]	Suction	0.1–7.9	7	54	1.49±2.00	5.00
Anopheles melas Theobald females[i]	Suction	0.1–7.9	7	24	1.05±1.77	4.43
Aedes albocephalus (Theobald)[i]	Suction	0.1–7.9	7	44	0.60±1.30	3.26
Culex thalassius Theobald males[i]	Suction	0.1–7.9	7	55	2.25±2.62	6.56
Culex thalassius Theobald females[i]	Suction	0.1–7.9	7	91	1.29±1.84	4.62
Diptera: Tephritidae						
Anastrepha ludens (Loew)[j]	G-yeast	0.1–3	4	240	1.58±0.62	1.55

Table 2 (continued)

Species	Trapping method[a]	Range of trap heights	Number of trap heights	Total catch[b]	Mean height of catch $\pm SD$	F_L (m)
Lepidoptera: Cossidae						
Prionoxystus robiniae Peck[k]	Bucket-P	1.5–9	4	160	4.42±2.93	7.34
Lepidoptera: Noctuidae						
Busseola fusca (Fuller)[l]	Funnel-P	0.5–2	4	(120)	1.34±0.48	1.20
Lepidoptera: Plutellidae						
Plutella xylostella (L.)[m]	Pherocon-P	0.3–1.5	3	170	0.37±0.20	0.51
Lepidoptera: Pyralidae						
Diaphania nitidalis (Stoll) males[n]	VF-bucket	0.3–1.8	4	188	1.12±0.42	1.06
Ostrinia nubilalis (Hübner)[o]	Light-UV	1.5–4.6	3	7172	2.55±1.17	2.93
Coniesta ignefusalis (Hampson)[p]	Water-P	0.1–2	4	392	0.30±0.30	0.76
Lepidoptera: Tortricidae						
Grapholitha molesta (Busck)[q]	Delta-P	1–4	3	427	2.72±1.03	2.58
Platynota flavedana Clemens[r]	Pherocon-P	0.3–3.9	5	850	1.79±0.95	2.38
Platynota idaeusalis (Walker)[r]	Pherocon-P	0.3–3.9	5	1817	1.88±0.98	2.45
Coleoptera: Chrysomelidae						
Diabrotica virgifera LeConte[s]	Pherocon-F	0–2.4	5	2235	0.96±0.72	1.80
Coleoptera: Curculionidae						
Cylas formicarius F.[t]	Funnel-P	0.09–0.85	7	3892	0.20±0.12	0.31
Coleoptera: Nitidulidae						
Glischrochilus quadrisignatus (Say)[u]	Bucket-d	0.3–5	5	3684	2.65±1.62	4.06
Glischrochilus fasciatus (Olivier)[u]	Bucket-d	0.3–5	5	1104	2.52±1.50	3.77
Carpophilus lugubris Murray[u]	Bucket-d	0.3–5	5	105	1.56±1.32	3.30
Coleoptera: Scarabaeidae						
Phyllopertha horticola L. males[v]	Y-X-vane-A	0.5–2	3	1119	1.14±0.57	1.43
Phyllopertha horticola L. females[v]	Y-X-vane-A	0.5–2	3	416	1.04±0.56	1.40
Popillia japonica Newman[w]	Y-floral	0.28–0.84	3	17175	0.52±0.22	0.54
Coleoptera: Scolytidae						
Hylurgops palliatus (Gryllenhal)[x]	St-screen	0.7–11.5	10	86	4.98±2.63	6.59
Ips typographus (L.)[x]	St-screen	0.7–11.5	10	103	4.63±2.75	6.89
Tomicus piniperda (L.)[x]	St-screen	0.7–11.5	10	10	5.98±3.00	7.53
Trypodendron domensticum (L.)[x]	St-screen	0.7–11.5	10	17	2.82±1.67	4.19
Cryphalus abietus (Ratz.)[x]	St-screen	0.7–11.5	10	242	3.44±2.73	6.84
Pityogenes bidentatus (Herbst)[x]	St-screen	0.7–11.5	10	23	3.10±1.62	4.06
Pityogenes chalcographus (L.)[x]	St-screen	0.7–11.5	10	84	6.89±2.90	7.27
Pityogenes quadridens (Hartig)[x]	St-screen	0.7–11.5	10	50	4.08±2.80	7.02
Hymenoptera: Agaonidae						
Elisabethiella baijnathi Wiebes[y]	St-cylinder	0.5–2	3	(100)	1.19±0.58	1.47
Phagoblastus barbarus Grandi[y]	St-cylinder	0.1–4.5	9	(419)	2.22±1.27	3.17
Hymenoptera: Braconidae						
Apanteles fumiferanae (Viereck) females[z]	Malaise	4.5–10	–	1455	7.35±1.46	3.67
Hymenoptera: Ichneumonidae						
Glypta fumiferanae (Viereck) females[z]	Malaise	4.5–10	–	1477	7.37±1.53	3.83

[a] Blue-St-card (blue sticky card); Y-St-card (yellow sticky card); W-St-card (white sticky card); Window (transparent window); St-cylinder (sticky plastic-cylinder); Suction (suction trap); G-yeast (Green food color and yeast hydrolysate in bucket trap); Bucket-P (sticky bucket with synthetic pheromone); Funnel-P (2-funnel trap with synthetic pheromone); Pherocon-P (Pherocon 1C trap with synthetic pheromone); VF-bucket (4 virgin females in bucket trap); Light-UV (UV light trap); Water-P (water trap with synthetic pheromone); Delta-P (Delta trap with synthetic pheromone); Pherocon-F (Pherocon 1C trap with synthetic floral attractants); Bucket-d (bucket trap with bread dough); Y-X-vane-A (yellow cross vanes with floral volatiles); Y-floral (yellow funnels with synthetic floral lure); St-screen (sticky screen cylinder); Malaise trap.

[b] Trap catch reported as proportions so catch in parentheses was assumed in order to calculate mean height of catch and variation.

[c] Gillespie and Vernon (1990).
[d] Diraviam and Uthamasamy (1992).
[e] Meyerdirk et al. (1979).
[f] McPherson and Weber (1990).
[g] McPherson et al. (1993).
[h] D'Arcy-Burt and Blackshaw (1987).
[i] Snow (1982).
[j] Robacker et al. (1990).
[k] Dix et al. (1979).
[l] Critchley et al. (1997).
[m] Chisholm et al. (1979).
[n] Valles et al. (1991).
[o] Ficht and Hienton (1941).
[p] Youm and Beevor (1995).
[q] Rothschild and Minks (1977).
[r] David and Horsburgh (1989).
[s] Weissling and Meinke (1991).
[t] Proshold et al. (1986).
[u] Peng and Williams (1991).
[v] Ruther (2004).
[w] Ladd and Klein (1982).
[x] Byers et al. (1989).
[y] Ware and Compton (1994).
[z] Elliott et al. (1986).

3.3. Simulation of insect movement and flight distribution in three dimensions

The interaction of SDA, $step$, and ω in producing normal distributions of desired SD appears complex. The best fit was usually found with $step = 0.1$ and $SDA = 6°$ (Table 3). Using these two parameters and varying SD and ω, a good fitting relationship was $\omega = 0.0715(SD)^{-0.9327}$ ($R^2 = 0.997$, $N = 6$). Simulations with 2000 insects each and $SD = 1$, $SDA = 6°$, $step = 0.1$ m, and $\omega = 0.0715$ gave a mean flight height of 4.999 ± 0.019 ($\pm 95\%$ C.L., $N = 8$). The same data were analyzed with the mean flight height method assuming all were caught on traps placed at the center of each of ten 1-m layers of the flight area (i.e., a trap at 0.5, 1.5, 2.5 m, etc.). This gave nearly an identical mean flight height of 4.9995 ± 0.02154 m with $SD = 1.0335 \pm 0.0106$. The numbers in 18 layers of the flight area usually were not significantly different from that expected of a normal distribution as shown by chi-square analysis, $\chi^2 = 21.3 \pm 11.62$ (12.09, 10.59, 19.00, 19.25, 53.87, 24.09, 13.09, 18.54), with seven of eight distributions not significantly different from a normal distribution.

3.4. Simulation of insect movement and catch on EAR in three dimensions

A spherical EAR of 0.5 m radius placed at the center of a $20\,\text{m} \times 20\,\text{m} \times 10\,\text{m}$ high simulation area caught 111.25 ± 8.47 of 2000 initial insects after they took 720 steps of 0.1 m each with $6°$ SDA (ω was 0.0715 radians) and distributed according to a normal distribution with mean of 5 m and $SD = 1$ m (Table 4). Based on a flight distribution with SD of 1 m, the calculated F_L was 2.51 m (Table 4). As the EAR was enlarged from 0.5 to 1 m radius within a flight density distribution of $SD = 1$ m, the catch increased from 111.25 to 364.13 due to more interception area. When the distribution was more diffuse at a larger SD of 1.67 m, the catch decreased and ranged from 69.25 to 236.00 as the EAR was similarly increased from 0.5 to 1 m (Table 4). When all 2000 insects were allowed to fly uniformly within a flight volume of height equal to F_L, then an equivalent number were caught compared to the normal distribution of flight within the 10-m high volume with appropriate SD and calculated F_L (Table 4). This indicates that Eq. (7) is valid for estimating the effective flight layer (F_L) that is needed in Eq. (5) to convert EAR to EAR_c.

3.5. Simulation of insect movement and catch on EAR_C in two dimensions

Eq. (5) predicts the EAR_c used in 2D models from a spherical EAR of catch measurements in the field and F_L of catch measurements on several trap heights. Simulations with the predicted EAR_c (Table 4) in 2D with the same 2000 insects showed that about the same number of insects were caught as that on the 3D spherical EAR. This confirms the validity of the conversion Eq. (5) and allows 2D simulation models of mass trapping and mating disruption based on field measurements of EAR (Byers, 2007, 2008).

Table 3
Observed standard deviation ($SD \pm 95\%$ C.L., $N = 8$) of vertical insect flight density of 2000 insects in a $20\,\text{m} \times 20\,\text{m} \times 10\,\text{m}$ volume after insects took 720 steps with various SDA of turning angles, step lengths, ω (see text), and specified SD

SDA, degrees	Step, m	ω, radians	Specified		Observed	
			SD, m	F_L, m	SD, m	F_L, m
6	0.10	0.1365	0.50	1.25	0.47 ± 0.01	1.19 ± 0.005
6	0.10	0.0715	1.00	2.51	0.99 ± 0.01	2.49 ± 0.03
6	0.10	0.0581	1.25	3.13	1.28 ± 0.02	3.21 ± 0.06
6	0.10	0.0440	1.67	4.18	1.68 ± 0.03	4.20 ± 0.07
6	0.10	0.0304	2.50	6.27	2.22 ± 0.03^{a}	5.57 ± 0.07
6	0.05	0.0400	1.00	2.51	0.98 ± 0.02	2.46 ± 0.04
12	0.15	0.1300	1.00	2.51	0.98 ± 0.02	2.46 ± 0.04
12	0.10	0.0900	1.00	2.51	1.03 ± 0.01	2.59 ± 0.04

[a] The specified and observed SD were different due to significant truncation of flight within the 10 m high layer.

Table 4
Catch ($\pm 95\%$ C.L., $N = 8$) in 3D volume ($20\,\text{m} \times 20\,\text{m} \times 10\,\text{m}$ high) on EAR at various standard deviations (SD) of normal distributions of flight and ω (see text) or at a uniform distribution in the effective flight layer, F_L, compared with catch in 2D area ($20\,\text{m} \times 20\,\text{m}$) on an equivalent EAR_c calculated from F_L (in all cases, insects took 720 steps, each 0.1 m with $6°$ SDA)

EAR, m	ω, radians	SD, m	F_L, m	3D catch on EAR	EAR_c, m	2D catch on EAR_c
Normal distribution of flight (within 10 m)						
0.50	0.0715	1.00	2.51	111.25 ± 8.47	0.1567	105.50 ± 6.97
0.50	0.0581	1.25	3.13	91.75 ± 8.56	0.1253	87.63 ± 9.76
0.50	0.0440	1.67	4.18	69.25 ± 8.94	0.0940	63.50 ± 6.37
0.75	0.0715	1.00	2.51	216.13 ± 8.72	0.3525	233.75 ± 15.74
0.75	0.0581	1.25	3.13	185.38 ± 13.88	0.2820	185.13 ± 14.65
0.75	0.0440	1.67	4.18	142.88 ± 5.20	0.2115	139.88 ± 11.10
1.00	0.0715	1.00	2.51	364.13 ± 14.34	0.6267	398.75 ± 19.27
1.00	0.0581	1.25	3.13	308.25 ± 17.06	0.5013	323.88 ± 15.59
1.00	0.0440	1.67	4.18	236.00 ± 12.98	0.3760	240.38 ± 7.15
Uniform distribution of flight (within F_L)						
0.50	–	–	2.51	105.75 ± 9.60	0.1567	105.88 ± 8.72
0.75	–	–	3.13	185.88 ± 12.95	0.2820	187.50 ± 8.56
1.00	–	–	4.18	242.88 ± 11.95	0.3760	243.88 ± 12.02

4. Discussion

Simulation models of mass trapping and mating disruption require knowledge about the magnitude of attraction of insects to semiochemical lures that catch insects or disrupt their attraction (Byers, 2007). One concept describing lure effect is the active space of plume area where male moths detect female moth pheromone (Sower et al., 1971; Nakamura and Kawasaki, 1977; Baker and Roelofs, 1981; Elkinton and Cardé, 1984). However, it has proven tedious and time-consuming to delineate the active space that is expected to change dynamically with time. In fact, this space is even more complicated because there are many varying source-finding probabilities or capture probabilities (CP) in the plume that are not practical to observe. Instead of modeling attraction of insects in a plume's active space, the EAR was proposed for use in simulation models (Byers, 1991, 1993, 1996, 2007). However, it was not clear whether an EAR could adequately substitute for the natural and complex plume response surfaces of which little is known.

The EAR as used originally (Byers et al., 1989) in Eq. (1), is calculated from the passive trap interception area as seen from a particular direction multiplied by the ratio of catch on the pheromone trap (A_c) and passive trap (P_c). Using a ratio of catches means that the EAR is relatively independent of population density and thus the EAR is a characteristic of the pheromone quality and release rate as well as the sensitively of the responding species. The interception area is solved for a circular area of radius EAR (also the radius of a sphere of this size). The EAR is useful to compare the relative strengths of semiochemical attractants among insect species and studies. An insect species with a larger EAR than a second species generally means that individuals of the first species are attracted from a longer distance, assuming the CP gradients in the two active spaces are about the same. The attractive trap must catch more than the passive trap, the passive trap should catch some insects, and higher catches on many passive traps will improve the accuracy of the EAR measurement. The attractive trap should be placed far enough from the passive trap as to hardly influence the latter's catch, but both kinds of traps should be within the same area of flight density. Estimating an EAR from published results is usually not possible because (a) the studies did not employ unattractive, blank traps to intercept flying insects, or (b) the blank traps did not catch insects. For example, most moth pheromone studies have used traps where moths must enter to be caught (e.g., Delta traps) and so very few are caught on blank traps (causing the EAR to be undefined).

The EAR can be purposively measured in the field using sticky traps. However, these EAR lures sample a portion of the flight layer (usually within meters of the ground for most agricultural insects) and thus when modeling in 2D it is necessary to convert the EAR to EAR_c (Byers, 2008). In order to do this, the effective flight layer must be estimated from catch on passive traps placed at various heights to obtain a mean flight height and SD. It was assumed that most insects have a density distribution when flying that is approximately normal, although many examples were found in the literature where densities appeared to increase with height. This undoubtedly occurred because not enough traps were placed high enough above ground to monitor a decline. Other examples were ignored because only one or two trap heights were used. Although few studies estimated mean flight height and SD, these were obtained from data in the literature on either proportions or numbers caught on traps at several heights. The number of trap levels increases the accuracy and confidence of the calculated values. The type of trap used to monitor flight height should not matter as long as they are the same and catch a correct proportion of flying insects at the respective heights. However,

many previous studies (Table 2) and reported in Byers (2008) have not used passive traps but rather attractive traps (e.g., yellow color, ultraviolet light, and sex/aggregation pheromone) that might alter the natural flight patterns. For example, the mean flight height of 4.63 m and SD of 2.75 m of the bark beetle, *Ips typographus* ($N = 103$), on sticky traps were lowered to a mean height of 1.50 and SD of 1.63 m ($N = 740$) by placing aggregation pheromone in the traps (Byers et al., 1989; Byers, 2008).

Once the SD is found for the mean flight height from traps at various heights, Eq. (7) is used to calculate an effective flight layer, F_L. In order to verify this equation, simulations were done in a $20 \times 20 \times 10$-m volume such that individual insects could fly anywhere but their population would distribute according to a mean flight height of 5-m with a normal distribution of specified SD (e.g. 1 m). Simulations of 2000 insects in the 10-m high volume with $SD = 1$ m allowed insects to be caught on a spherical EAR over a certain duration. The same number of insects flying in a uniform distribution within a volume of height F_L over the duration gave the same equivalent catch on the spherical EAR as that in the 10-m high volume with normal distribution of insect flight density, indicating that Eq. (7) is valid. The F_L can then be used in Eq. (5) to convert the spherical EAR to the 2D circular EAR_c.

Recently, simulations demonstrated that males encountering CP-active space plumes of a specific dimension in 2D reach the pheromone source at a rate that was equivalent to a circular EAR_c of appropriate size (Byers, 2008). Thus, modeling insect encounter-rates with the EAR_c is more easily accomplished than attempting to model such rates with a CP-active space plume. In the present study, the spherical EAR in 3D simulations with 2000 insects in a $20\,m \times 20\,m \times 10\,m$ volume caught an equivalent number of insects as did the transformed circular EAR_c in 2D simulations with the same insects in a $20\,m \times 20\,m$ area, indicating that Eq. (5) also is valid.

Models are useful to both better understand and predict efficiency of mating disruption and mass trapping of pest insects with competitive attraction and camouflage (Byers, 2007). In the case of moths, key parameters include male search, female calling, insect and dispenser densities, and EAR_c of females and dispensers. However, many of these parameters are difficult to quantify in nature for a particular pest species, for example, moth density and male search distance. Other parameters, although usually not measured, can be estimated more easily such as EAR of females and EAR of dispensers by using catch ratios on sticky traps and converting to EAR_c with F_L estimated from sticky trap catches at fixed heights.

References

Adams, L., 1987. High Performance Interactive Graphics. Tab Books, Blue Ridge Summit, PA.

Baker, T.C., Roelofs, W.L., 1981. Initiation and termination of oriental fruit moth male response to pheromone concentrations in the field. Environ. Entomol. 10, 211–218.

Baker, T.C., Fadamiro, H., Cossé, A.A., 1998. Fine-grained resolution of closely spaced odor strands by flying male moths. Nature 393, 530.

Bossert, W.H., Wilson, E.O., 1963. The analysis of olfactory communication among animals. J. Theor. Biol. 5, 443–469.

Branco, M., Jactel, H., Franco, J.C., Mendel, Z., 2006. Modelling response of insect trap captures to pheromone dose. Ecol. Model. 197, 247–257.

Byers, J.A., 1983. Sex-specific responses to aggregation pheromone: regulation of colonization density in the bark beetle *Ips paraconfusus*. J. Chem. Ecol. 9, 129–142.

Byers, J.A., 1987. Interactions of pheromone component odor plumes of western pine beetle. J. Chem. Ecol. 13, 2143–2157.

Byers, J.A., 1991. Simulation of mate-finding behaviour of pine shoot beetles, *Tomicus piniperda*. Anim. Behav. 41, 649–660.

Byers, J.A., 1993. Simulation and equation models of insect population control by pheromone-baited traps. J. Chem. Ecol. 19, 1939–1956.

Byers, J.A., 1996. An encounter rate model for bark beetle populations searching at random for susceptible host trees. Ecol. Model. 91, 57–66.

Byers, J.A., 1999. Effects of attraction radius and flight paths on catch of scolytid beetles dispersing outward through rings of pheromone traps. J. Chem. Ecol. 25, 985–1005.

Byers, J.A., 2001. Correlated random walk equations of animal dispersal resolved by simulation. Ecology 82, 1680–1690.

Byers, J.A., 2007. Simulation of mating disruption and mass trapping with competitive attraction and camouflage. Environ. Entomol. 36, 1328–1338.

Byers, J.A., 2008. Active space of pheromone plume and its relationship to effective attraction radius in applied models. J. Chem. Ecol. 34, 1134–1145.

Byers, J.A., Lanne, B.S., Löfqvist, J., Schlyter, F., Bergström, G., 1985. Olfactory recognition of host-tree susceptibility by pine shoot beetles. Naturwissenschaften 72, 324–326.

Byers, J.A., Birgersson, G., Löfqvist, J., Bergström, G., 1988. Synergistic pheromones and monoterpenes enable aggregation and host recognition by a bark beetle. Naturwissenschaften 75, 153–155.

Byers, J.A., Anderbrant, O., Löfqvist, J., 1989. Effective attraction radius: a method for comparing species attractants and determining densities of flying insects. J. Chem. Ecol. 15, 749–765.

Cardé, R.T., 1990. Principles of mating disruption. In: Ridgway, R.L., Silverstein, R.M. (Eds.), Behavior-Modifying Chemicals for Pest Management: Applications of Pheromones and other Attractants. Marcel Dekker, New York, pp. 47–71.

Chisholm, M.D., Underhill, E.W., Steck, W.F., 1979. Field trapping of the diamondback moth Plutella xylostella using synthetic sex attractants. Environ. Entomol. 8, 516–518.

Critchley, B.R., Hall, D.R., Farman, D.I., McVeigh, L.J., Mulaa, M.A.O.A., Kalama, P., 1997. Monitoring and mating disruption of the maize stalkborer, Busseola fusca, in Kenya with pheromones. Crop Prot. 16, 541–548.

D'Arcy-Burt, S., Blackshaw, R.P., 1987. Effects of trap design on catches of grassland Bibionidae (Diptera: Nematocera). Bull. Entomol. Res. 77, 309–315.

David, P.J., Horsburgh, R.L., 1989. Effects of pheromone trap design, placement, and pheromone dispenser and load on male Platynota flavedana and P. idaeusalis (Lepidoptera: Tortricidae) catches in Virginia apple orchards. Environ. Entomol. 18, 145–149.

Diraviam, J., Uthamasamy, S., 1992. Monitoring whitefly, Bemisia tabaci (Genn.) on sunflower with yellow sticky traps. J. Entomol. Res. 16, 163–165.

Dix, M.E., Solomon, J.D., Doolittle, R.E., 1979. Influences of pheromone dispenser and trap placement on trapping carpenterworm moths in North Dakota and Mississippi. Environ. Entomol. 8, 322–325.

El-Sayed, A.M., Suckling, D.M., Wearing, C.H., Byers, J.A., 2006. Potential of mass trapping for long-term pest management and eradication of invasive species. J. Econ. Entomol. 99, 1550–1564.

Elkinton, J.S., Cardé, R.T., 1984. Odor dispersion. In: Bell, W.J., Cardé, R.T. (Eds.), Chemical Ecology of Insects. Sinauer Associates, Inc., Sunderland, MA, pp. 73–91.

Elkinton, J.S., Cardé, R.T., Mason, C.J., 1984. Evaluation of time-averaged dispersion models for estimating pheromone concentration in a deciduous forest. J. Chem. Ecol. 10, 1081–1108.

Elliott, N.C., Simmons, G.A., Drapek, R.J., 1986. Adult emergence and activity patterns of parasites of early instar jack pine budworm (Lepidoptera: Tortricidae). Environ. Entomol. 15, 409–416.

Fares, Y., Sharpe, P.J.H., Magnuson, C.E., 1980. Pheromone dispersion in forests. J. Theor. Biol. 84, 335–359.

Ficht, G.A., Hienton, T.E., 1941. Some of the more important factors governing the flight of European corn borer moths to electic traps. J. Econ. Entomol. 34, 599–604.

Gara, R.I., 1963. Studies on the flight behavior of Ips confuses (Lec.) (Coleoptera: Scolytidae) in response to attractive material. Contrib. Boyce Thompson Inst. 22, 51–66.

Gillespie, D.R., Vernon, R.S., 1990. Trap catch of western flower thrips (Thysanoptera: Thripidae) as affected by color and height of sticky traps in mature greenhouse cucumber crops. J. Econ. Entomol. 83, 971–975.

Hearn, D., Baker, M.P., 1994. Computer Graphics. Prentice Hall, Englewood Cliffs, NJ.

Ladd Jr., T.L., Klein, M.G., 1982. Japanese beetle (Coleoptera: Scarabaeidae): effect of trap height on captures. J. Econ. Entomol. 75, 746–747.

Mankin, R.W., Vick, K.W., Mayer, M.S., Coffelt, J.A., Callahan, P.S., 1980. Models for dispersal of vapors in open and confined spaces: applications to sex pheromone trapping in a warehouse. J. Chem. Ecol. 6, 929–950.

McCall, R.B., 1970. Fundamental Statistics for Psychology. Harcourt, Brace and World, Inc., New York.

McClendon, R.W., Mitchell, E.B., Jones, J.W., McKinion, J.M., Hardee, D.D., 1976. Computer simulation of pheromone trapping systems as applied to boll weevil population suppression: a theoretical example. Environ. Entomol. 5, 799–806.

McPherson, J.E., Weber, B.C., 1990. Seasonal flight patterns of Hemiptera (excluding miridae) in a southern Illinois black walnut plantation. Great Lakes Entomol 23, 105–120.

McPherson, J.E., Weber, B.C., Henry, T.J., 1993. Seasonal flight patterns of Miridae (Hemiptera) in a southern Illinois black walnut plantation. Great Lakes Entomol 26, 97–106.

Meyerdirk, D.E., Hart, W.G., Burnside, J.A., 1979. Flight behavior of the citrus blackfly. J. Econ. Entomol. 72, 395–398.

Miller, J.R., Gut, L.J., de Lame, F.M., Stelinski, L.L., 2006a. Differentiation of competitive vs. non-competitive mechanisms mediating disruption of moth sexual communication by point sources of sex pheromone (part 1): Theory. J. Chem. Ecol. 32, 2089–2114.

Miller, J.R., Gut, L.J., de Lame, F.M., Stelinski, L.L., 2006b. Differentiation of competitive vs. non-competitive mechanisms mediating disruption of moth sexual communication by point sources of sex pheromone (part 2): case Studies. J. Chem. Ecol. 32, 2115–2143.

Nakamura, K., Kawasaki, K., 1977. The active space of the Spodoptera litura (F.) sex pheromone and the pheromone component determining this space. Appl. Entomol. Zool. 12, 162–177.

Peng, C., Williams, R.N., 1991. Effect of trap design, trap height, and habitat on the capture of sap beetles (Coleoptera: Nitidulidae) using whole-wheat bread dough. J. Econ. Entomol. 84, 1515–1519.

Proshold, F.I., Gonzalez, J.L., Asencio, C., Heath, R.R., 1986. A trap for monitoring the sweetpotato weevil (Coleoptera: Curculionidae) using pheromone or live females as bait. J. Econ. Entomol. 79, 641–647.

Robacker, D.C., Moreno, D.S., Wolfenbarger, D.A., 1990. Effects of trap color, height, and placement around trees on capture of Mexican fruit flies (Diptera: Tephritidae). J. Econ. Entomol. 83, 412–419.

Rothschild, G.H.L., Minks, A.K., 1977. Some factors influencing the performance of pheromone traps for oriental fruit moth in Australia. Entomol. Exp. Appl. 22, 171–182.

Ruther, J., 2004. Male-biassed response of garden chafer, Phyllopertha horticola L., to leaf alcohol and attraction of both sexes to floral plant volatiles. Chemoecology 14, 187–192.

Schlyter, F., Byers, J.A., Löfqvist, J., 1987. Attraction to pheromone sources of different quantity, quality, and spacing: density-regulation mechanisms in bark beetle Ips typographus. J. Chem. Ecol. 13, 1503–1523.

Snow, W.F., 1982. Further observations on the vertical distribution of flying mosquitoes (Diptera: Culicidae) in West African savanna. Bull. Entomol. Res. 72, 695–708.

Sower, L.L., Gaston, L.K., Shorey, H.H., 1971. Sex pheromones of noctuid moths. XXVI. Female release rate, male response threshold, and communication distance for Trichoplusia ni. Ann. Entomol. Soc. Am. 64, 1448–1456.

Sutton, O.G., 1953. Micrometeorology. McGraw-Hill, New York.

Turchin, P., 1998. Quantitative Analysis of Movement. Sinauer Associates, Inc., Sunderland, MA.

Valles, S.M., Capinera, J.L., Teal, P.E.A., 1991. Evaluation of pheromone trap design, height, and efficiency for capture of male Diaphania nitidalis (Lepidoptera: Pyralidae) in a field cage. Environ. Entomol. 20, 1274–1278.

Wall, C., Perry, J.N., 1987. Range of action of moth sex-attractant sources. Entomol. Exp. Appl. 44, 5–14.

Ware, A.B., Compton, S.G., 1994. Dispersal of adult fig wasps. 2. Movements between trees. Entomol. Exp. Appl. 73, 231–238.

Weissling, T.J., Meinke, L.J., 1991. Semiochemical-insecticide bait placement and vertical distribution of corn rootworm (Coleoptera: Chrysomelidae) adults: implications for management. Environ. Entomol. 20, 945–952.

Youm, O., Beevor, P.S., 1995. Field evaluation of pheromone-baited traps for Coniesta ignefusalis (Lepidoptera: Pyralidae) in Niger. J. Econ. Entomol. 88, 65–69.